

Optimal electron, phonon, and magnetic characteristics for low energy thermally induced magnetization switching

ATXITIA, U., OSTLER, Thomas <<http://orcid.org/0000-0002-1328-1839>>, CHANTRELL, R. W. and CHUBYKALO-FESENKO, O.

Available from Sheffield Hallam University Research Archive (SHURA) at:

<https://shura.shu.ac.uk/15273/>

This document is the Published Version [VoR]

Citation:

ATXITIA, U., OSTLER, Thomas, CHANTRELL, R. W. and CHUBYKALO-FESENKO, O. (2015). Optimal electron, phonon, and magnetic characteristics for low energy thermally induced magnetization switching. *Applied Physics Letters*, 107 (19), p. 192402. [Article]

Copyright and re-use policy

See <http://shura.shu.ac.uk/information.html>

Optimal electron, phonon, and magnetic characteristics for low energy thermally induced magnetization switching

U. Atxitia, T. A. Ostler, R. W. Chantrell, and O. Chubykalo-Fesenko

Citation: [Applied Physics Letters](#) **107**, 192402 (2015); doi: 10.1063/1.4935416

View online: <http://dx.doi.org/10.1063/1.4935416>

View Table of Contents: <http://scitation.aip.org/content/aip/journal/apl/107/19?ver=pdfcov>

Published by the [AIP Publishing](#)

Articles you may be interested in

[Ultrafast spin-switching of a ferrimagnetic alloy at room temperature traced by resonant magneto-optical Kerr effect using a seeded free electron laser](#)

[Rev. Sci. Instrum.](#) **86**, 083901 (2015); 10.1063/1.4927828

[Ultrafast thermally induced magnetic switching in synthetic ferrimagnets](#)

[Appl. Phys. Lett.](#) **104**, 082410 (2014); 10.1063/1.4867015

[Thermal stability of pinned synthetic ferrimagnets with perpendicular magnetic anisotropy](#)

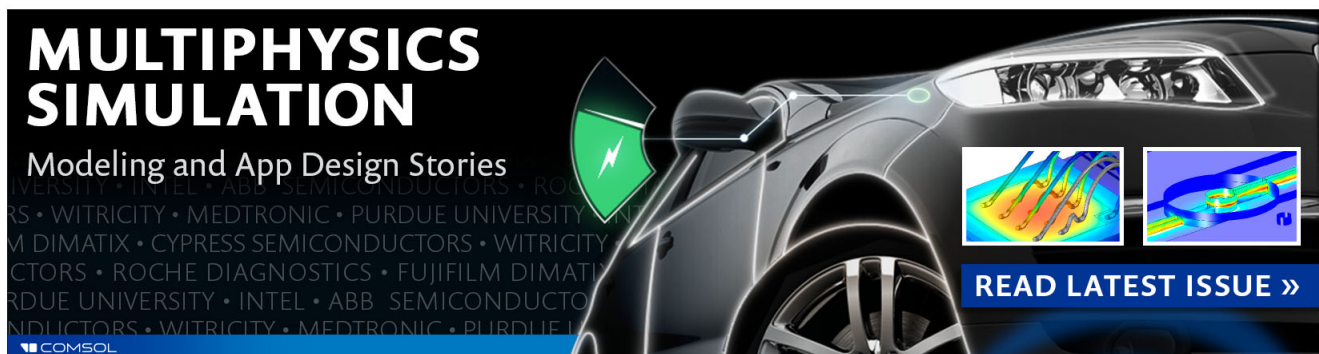
[J. Appl. Phys.](#) **95**, 7163 (2004); 10.1063/1.1687534

[Thermal dependence of magnetic springs location in a DyFe 2 / YFe 2 superlattice](#)

[J. Appl. Phys.](#) **95**, 6843 (2004); 10.1063/1.1687202

[T-induced changes of magnetization profiles and reversal in exchange-coupled trilayers](#)

[J. Appl. Phys.](#) **85**, 5974 (1999); 10.1063/1.370505

The advertisement features a dark background with a sleek, modern car on the right side. On the left, the text 'MULTIPHYSICS SIMULATION' is written in large, bold, white capital letters. Below it, 'Modeling and App Design Stories' is written in a smaller white font. A green lightning bolt icon is positioned to the left of the car. Two small inset images show simulation results: one with a color gradient and another with a blue and yellow pattern. At the bottom right, a blue button with white text says 'READ LATEST ISSUE >>'. The COMSOL logo is visible in the bottom left corner.

**MULTIPHYSICS
SIMULATION**
Modeling and App Design Stories

READ LATEST ISSUE >>

COMSOL

Optimal electron, phonon, and magnetic characteristics for low energy thermally induced magnetization switching

U. Atxitia,^{1,2,a),b)} T. A. Ostler,^{3,4,c)} R. W. Chantrell,³ and O. Chubykalo-Fesenko⁵

¹Fachbereich Physik, Universität Konstanz, D-78457 Konstanz, Germany

²Zukunftskolleg, Universität Konstanz, D-78457 Konstanz, Germany

³Department of Physics, University of York, York YO105DD, United Kingdom

⁴College of Engineering, Mathematics and Physical Sciences, University of Exeter, Exeter, Devon EX4 4SB, United Kingdom

⁵Instituto de Ciencia de Materiales de Madrid, CSIC, Cantoblanco, 28049 Madrid, Spain

(Received 10 August 2015; accepted 27 October 2015; published online 9 November 2015)

Using large-scale computer simulations, we thoroughly study the minimum energy required to thermally induced magnetization switching (TIMS) after the application of a femtosecond heat pulse in transition metal-rare earth ferrimagnetic alloys. We find that for an energy efficient TIMS, a low ferrimagnetic net magnetization with a strong temperature dependence is the relevant factor for the magnetic system. For the lattice and electron systems, the key physics for efficient TIMS is a large electron-phonon relaxation time. Importantly, we show that as the cooling time of the heated electrons is increased, the minimum power required to produce TIMS can be reduced by an order of magnitude. Our results show the way to low power TIMS by appropriate engineering of magnetic heterostructures. © 2015 AIP Publishing LLC. [<http://dx.doi.org/10.1063/1.4935416>]

Manipulation of magnetization without the need for magnetic fields has attracted much attention in the last few decades in many fields, such as spintronics,¹ electric field manipulation of magnetism,² acousto-magneto-plasmonics,³ caloritronics,⁴ or femtosecond laser physics.⁵ Driven by the possibilities of low-power magnetization manipulation at the ultrashort time scale, the laser induced magnetization switching, named *all-optical switching* (AOS),⁶ has recommended itself as a promising technique for technological purposes, from magnetic data storage⁷ to all-optical interconnects.⁸ The application of a single femtosecond laser pulse to ferrimagnetic alloys reverses its magnetic state in the picosecond time scale,⁶ where the underlying physical mechanism has a purely thermal origin.^{7,9–11} As a consequence, it has been called thermally induced magnetization switching (TIMS).^{12,13} Moreover, it has been recently shown to be a very low power mechanism for magnetic bit recoding with prospective to consume as low as 10 fJ per 10 nm² bit¹⁰ in comparison to the low-power spintronic memories still in development, where the spin transfer torque random access memories (RAM) could consume as little as 100 fJ/bit, and prospects indicate that electric-field-controlled magnetoelectric RAM will consume around 10 fJ/bit.¹⁴ However, we note here that differently to the slow magnetic-field driven magnetic reversal,¹⁵ the Landauer limit is still far from being achieved in TIMS. Although the energy required to reverse the magnetization is low, the temperature after the switching remains for a few hundreds of picoseconds rather high, even close to the Curie temperature (T_c), before complete dissipation to the environment. Thus, lowering the fluence required to reverse the magnetic state of a material by TIMS will not

only allow one to realize an ultra-low power magnetic bit-recording scheme but also to avoid the inconvenient long lasting elevated temperatures.

To do so, one needs a good knowledge of the physical mechanisms involved, non-equilibrium dynamics of the spin system, electrons and lattice vibrations (phonons). However, little is known about the effect of electron and phonon characteristics on TIMS since previous theoretical works^{12,16–18} in the literature have focused on the fundamental question of which magnetic mechanism produces TIMS.

The optimum properties of the magnetic system for TIMS are still the subject of debate in the literature.^{19,20} Initial experimental observations highlighted the importance of the magnetization compensation temperature,²¹ T_M , where the net magnetization, $M_{\text{net}}(T)$, of the magnet is zero but the element specific magnetization remains finite. Further experiments have shown that the existence of T_M is not completely necessary, but low $M_{\text{net}}(T)$ criteria is more adequate.^{20,22} A theoretical work by Barker and co-workers¹² presented a microscopic view based on a non-equilibrium energy transfer between the ferro- and antiferromagnetic like magnon branches, and suggests that TIMS is not restricted to be around the compensation temperature (low remanence); however, the laser energy needed to produce TIMS is minimum around T_M . Atxitia *et al.*²³ showed that the distinct element specific demagnetization rate is related to the shape of the equilibrium magnetization curve, suggesting that a strong temperature dependence of the net magnetization is necessary.

From these experimental and theoretical works, one can extract three basic ingredients that lead to magnetization switching in two element ferrimagnets: (i) AFM coupling, (ii) low net magnetization at remanence, and (iii) distinct element specific demagnetization dynamics. Recently, Mangin and co-workers¹⁹ has been able to show all optical switching with circularly polarized laser pulses in a range of materials,

^{a)} Author to whom correspondence should be addressed. Electronic mail: Unai.Atxitia@uni-konstanz.de

^{b)} U. Atxitia and T. A. Ostler contributed equally to this work.

^{c)} Electronic mail: t.ostler@exeter.ac.uk

TABLE I. Parameters utilised in the two temperature model in Eqs. (1) and (2).

TTM	
Electronic heat capacity	$C_e = \gamma_e T_e, \gamma_e = 2.25 \times 10^2 \text{ Jm}^3\text{K}^{-1}$
Phonon specific heat	$C_{\text{ph}} = 3.1 \times 10^6 \text{ Jm}^3$
Electron-phonon coupling	G_{ep} variable
Laser duration	$\tau_p = 50 \text{ fs}$
Laser energy input	$P(t_0, \tau_p) = P_0 \exp(-(t/\tau_p)^2)$
Pulse fluence	$F_0 = P_0 \tau_p \sqrt{\pi}$

from alloys to rare earth free AFM coupled multilayers, partially based on the above mentioned design rules. Thus, these rules or criteria are very useful to find or engineer materials showing TIMS; however, it is difficult to infer from them the optimum properties for a low energy consuming TIMS. In addition, no reference to the effect of the electron and lattice dynamics is given by these criteria. In this work, we perform a systematic study of the optimum properties of the spin, electron, and lattice systems to obtain the magnetization switching with the minimum laser energy possible.

We show that as the cooling time of the heated electrons is increased, the minimum power required to produce TIMS can be reduced by an order of magnitude. In particular, since this cooling time is driven by the electron-phonon interaction, materials with low electron-phonon coupling are therefore predicted to need much less laser fluence to exhibit TIMS.

For the simulations of the spin dynamics, we use the atomistic stochastic Landau-Lifshitz-Gilbert equation resting in a semi-classical spin Heisenberg Hamiltonian as presented and used in several previous works.^{9,24,25} The system size was $100 \times 100 \times 100$ spins on a simple cubic lattice, and so, the errors in the switching probability are quite low.

The effect of the femtosecond laser pulses on the electron and phonon dynamics is well described by the two-temperature model (2TM)²⁶ [see Table I for parameter definition and values used for GdFeCo, and Fig. 1(a)]

$$C_e(T_e) \frac{dT_e}{dt} = G_{\text{ep}}(T_e - T_{\text{ph}}) + P_0(t), \quad (1)$$

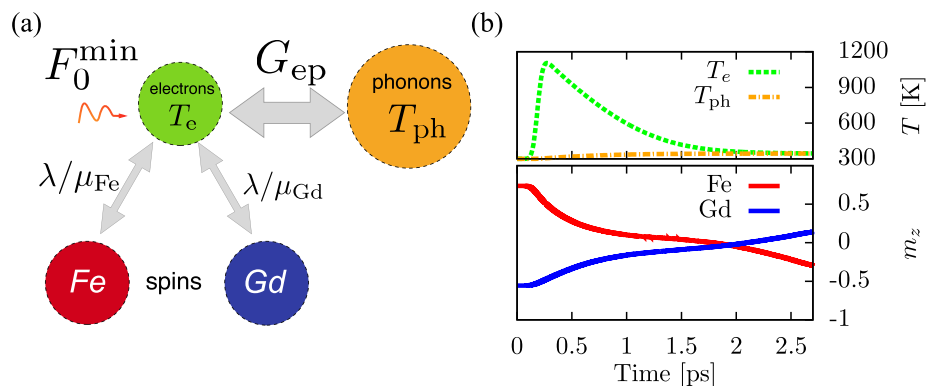


FIG. 1. (a) Schematic of the energy exchange between systems in the laser induced magnetization switching process. The laser energy F_0^{min} is absorbed by the electron system. The excess of energy of the electron system is transferred to the phonon system at a rate defined by the electron-phonon coupling, G_{ep} , and to the spin system at a rate determined by the ratio between the damping constant, λ , and the atomic magnetic moment, $\mu_{\text{Fe(Gd)}}$. (b) (Top) Electron and phonon temperature transients after the application of heat pulse, (bottom) and the element specific dynamics of the z - component of the magnetization showing the magnetization switching.

$$C_{\text{ph}} \frac{dT_{\text{ph}}}{dt} = -G_{\text{ep}}(T_e - T_{\text{ph}}). \quad (2)$$

The 2TM assumes that the energy from the laser pulse, represented by $P_0(t) = F_0/\tau_p\sqrt{\pi}$, is absorbed by the electron system, which thermalizes to an internal quasi-equilibrium distribution with a well-defined transient temperature $T_e(t)$. The initial temperature was set to ambient, $T = 300 \text{ K}$, since it is convenient to work at room temperature for technological purposes. The fluence P_0 was varied to find the minimum fluence, $F_0^{\text{min}} = P_0^{\text{min}}\tau_p\sqrt{\pi}$ required for switching, and the data sets were averaged over 10 runs with different random number seeds. Due to the usual low electron heat capacity, the maximum temperatures could go up to thousands of Kelvin. At the same time, the phonon temperature $T_{\text{ph}}(t)$ remains low; thus, the distortion of the electronic cloud and the excitation of the phonon modes gives rise to a non-equilibrium energy transfer between electrons and the lattice. The electron-phonon coupling, G_{ep} , drives both systems to a common temperature in the time scale of a few picoseconds [see Fig. 1(b)].

The minimum fluence F_0^{min} required to switch the magnetization, after a single laser pulse, depends significantly on the alloy composition and a minimum appears at Gd concentrations around 30% [Fig. 2 (right)]. For a Gd concentration of $x = 25\%$, the magnetization compensation point is located at room temperature [see Fig. 2 (Left)], and thus satisfying very closely the criteria of low net magnetization. The minimum fluence to TIMS of the $x = 25\%$ alloys is higher than the required to switch alloys of $x = 30\%$. The $x = 30\%$ alloy has a compensation temperature far above room temperature, $T_M = 425 \text{ K}$. This result is somehow contradictory in terms of solely the low magnetization criteria. This apparent contradiction can be resolved when one takes into account the TIMS requirement of differential sublattice demagnetization rates, related²³ to the temperature dependence of $M_{\text{net}}(T)$. Fig. 2 (left) shows that the temperature derivative of the magnetization for $x = 30\%$ is larger than that of $x = 25\%$, suggesting that for $x = 30\%$, the non-equivalence between sub-lattices is larger, compensating for the increased magnetization value. For $x = 20\%$, although the net magnetization is similar to $x = 30\%$, the F_0^{min} is a factor of 1.6 higher.

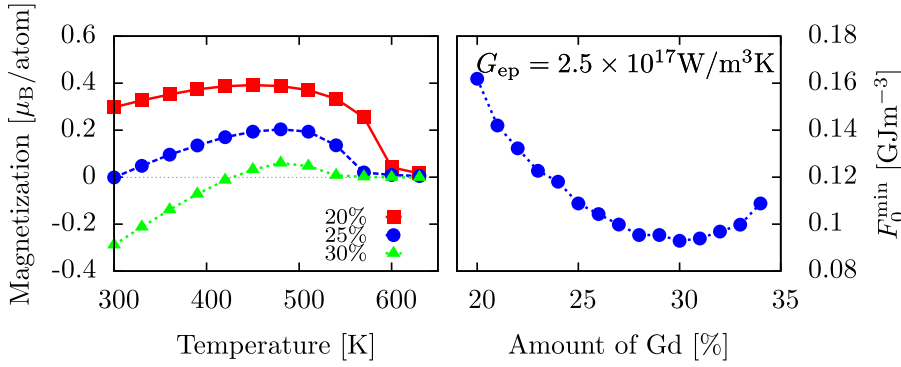


FIG. 2. (Left) Equilibrium magnetization gained from atomistic spin model simulations of $\text{Gd}_x(\text{FeCo})_{1-x}$ alloys with $x=20, 25$ and 30% . The compensation temperature, where $M_{\text{net}}(T_M) = 0$, lies around 425 K for $x = 30\%$ and 300 K for $x = 25\%$. (Right) Minimal fluence required for magnetization switching via TIMS as a function of composition, damping parameter $\lambda = 0.02$.

Again, the temperature dependence of $M_{\text{net}}(T)$ in both cases is very dissimilar, with $x = 20\%$ showing a less pronounced T dependence than $x = 30\%$. From our results, we conclude that the non-equivalence criteria are relatively more important for TIMS than the low magnetization one. So far, this criterion has not been used to interpret experimental results in the literature. We note that the temperature derivative of the magnetization has been shown²³ to qualitatively describe the sublattice relaxation times, so here we choose to highlight $dM_{\text{net}}(T)/dT$ as a criterion for TIMS since it is a more accessible measurement than the use of XMCD which was used to establish the differential relaxation rates.²⁵

To find ferrimagnets with enhanced differential sublattice relaxation rates, for example, in synthetic ferrimagnets or superlattices, the following recipe can be followed: the intra-sublattice exchange of one species must be much higher than the other, $J_{ij}^{\text{AA}} \gg J_{ij}^{\text{BB}}$ whilst simultaneously possessing a significantly lower atomic magnetic moment, $\mu_A < \mu_B$. This is indeed the case for rare earth (high μ and low J) coupled to transition metals (relatively low μ and high J), although upon alloying the values of J_{ij}^{AA} and J_{ij}^{BB} can change and in the case of amorphous alloys become more close to each other. This smearing out can be partially avoided for a bilayer composed of pure elements at each layer and therefore the differential sublattice demagnetization will be enhanced with respect to the alloys. Experiments on rare earth transition metal multilayers are still at an early stage, the helicity dependent all-optical switching has been observed in several rare-earth transition metal alloys.¹⁹ We note that the inter-sublattice coupling should not be too strong to avoid overly rigid motion of the sublattices.

We now focus our attention on the role of the electron and phonon systems on the power required for reversing the magnetization by a laser pulse. To do so, we consider the magnetic system parameters fixed to those corresponding to $x = 30\%$ [see Fig. 2], which requires the lowest power to switch the magnetization. We also fix the electron and phonon heat capacity. Whereas the values of the electron and phonon specific heat are rather well known, it is not the case for the electron-phonon coupling, G_{ep} , in ferromagnetic metals, such as the transition metals Ni, Fe, Co, and alloys based on them. The G_{ep} is however better known in rare earth metals. The exact value of G_{ep} for GdFeCo alloys is unknown; however, in recent works,^{12,18,23} where the ultrafast magnetization dynamics of GdFeCo was modelled, a value of $G_{\text{ep}} = 17.5 \times 10^{17} \text{Wm}^{-3}\text{K}^{-1}$ has been consistently used. Thus, no theoretical or computational result of the effect of

G_{ep} has been presented so far in the literature. In our simulations, the electron-phonon coupling is then varied from a very low value of $G_{\text{ep}} = 1 \times 10^{17} \text{Wm}^{-3}\text{K}^{-1}$, consistent with pure Gd,²⁷ intermediate ones corresponding to Fe and Fe alloys, to high values of $G_{\text{ep}} = 35 \times 10^{17} \text{Wm}^{-3}\text{K}^{-1}$ associated with Co and its alloys. This is consistent with *ab-initio* calculations where it has been shown that the localized d states feel stronger effect from the excitation of a phonon mode,²⁸ thus making the G_{ep} for Co/Co alloys consistently larger than those for Fe/Fe alloys. This trend can be observed in Figure 3 (bottom) which shows the maximum and minimum values for G_{ep} collected from literature.

The minimum fluence F_0^{\min} to switch the magnetization increases almost linearly as a function of G_{ep} [see Figure 3]. The electron-phonon coupling (G_{ep}) controls the rate at which the hot electrons cool by transferring energy to the phonon bath. As G_{ep} increases, this energy transfer becomes faster and thus the electron cooling time is shortened; consequently, the maximum temperature T_{max} is also reduced.

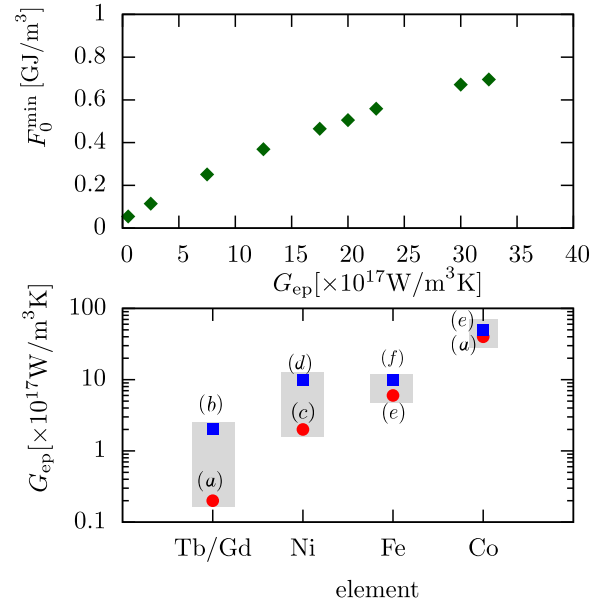


FIG. 3. (Top) F_0^{\min} minimum as a function of G_{ep} . (Bottom) Maximum (blue squares) and minimum (red circles) values of G_{ep} from literature: (a) Reference 29, (b) Reference 27, (c) Reference 30, (d) Reference 31, (e) Reference 28, and (f) Reference 32. In Ref. 28, instead of the macroscopic electron-phonon coupling, G_{ep} , the microscopic electron-phonon interaction, $\lambda_{\text{e-ph}}$, is calculated. To transform from microscopic, $\lambda_{\text{e-ph}}$, to macroscopic, G_{ep} , we have used the relation $G_{\text{ep}} = \pi \hbar k_{\text{B}} \lambda_{\text{e-ph}} (\theta_{\text{D}} (k_{\text{B}}/\hbar))^2 g(E_{\text{F}})/2$,³⁰ where θ_{D} is the Debye temperature, and $g(E_{\text{F}})$ the density of states at the Fermi level.²⁸

Therefore, for high G_{ep} , the thermal energy available to the spin system is smaller; therefore, the minimum F_0^{\min} increases in order to provide the same energy. This is in agreement with the theoretical prediction by Barker *et al.*,¹² where it is proven that a minimum amount of extra energy from the laser is necessary to excite both the ferro- and antiferro-magnetic like magnon branches, which ultimately drives the magnetization reversal. This extra energy is more efficiently pumped to the spin system if the electron temperature remains high for longer times. It remains a challenge to find ferrimagnetic materials that demonstrate TIMS but have low values of the electron-phonon coupling; however, still little is known about the precise value of the electron-phonon coupling in these complex ferrimagnetic alloys.

As well as investigating the effect of the composition and electron-phonon coupling on the fluence required for switching, we have also studied the minimum fluence F_0^{\min} required for TIMS as a function of the microscopic coupling to the thermal bath, λ [Fig. 4]. In previous computational works a value of $\lambda = 0.02$ was used, here we systematically vary λ around values consistent with experimental observations, $\lambda = 0.01 - 0.07$. We observe that the reduction of the required fluence with increasing damping [Fig. 4] is associated to the increase of the rate of exchange of energy by the magnetic system and the heat-bath. Specifically, the presence of higher damping values means an increase in the spin-flip scattering rate³³ and in terms of energy absorption by the magnetic subsystems means that the excitation of non-equilibrium states leading to TIMS¹² can be accessed more effectively with lower transient electron temperatures (laser pulse energies).

To summarise, we have found clear and simple material parameter criteria to excite TIMS for the important properties affecting the magnetic system (composition, temperature, and coupling), consistent with previous experimental studies, to obtain an ultra-low energy TIMS. The magnetic system, besides being ferrimagnetic, should present a low net magnetization at operating temperature and the electron and phonon systems should have a weak electron-phonon interaction. Within these conditions, we can predict that Co and Co-based alloys (or heterostructures) are not the best candidates for an energy efficient TIMS due to the expected high electron-phonon coupling. We note that pure cobalt has a high Curie temperature, thus by fabricating multilayers of Co and another low Curie temperature ferromagnet, the

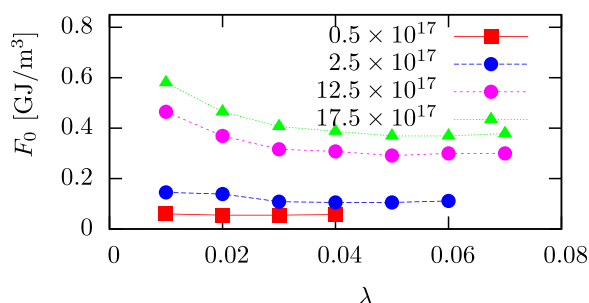


FIG. 4. Fluence threshold to TIMS as a function of the coupling to the bath parameter, λ , for four characteristic values of the electron-phonon coupling parameter.

proposed non-equivalence criteria (large $M(T)$ temperature derivative) could be easily fulfilled and even enhanced, leading to a low energy TIMS. As for Fe and Fe based materials, our results suggest that these are well positioned for low energy TIMS since they present an intermediate electron-phonon coupling.

With this study, we have brought additional insights into TIMS that could help with the optimisation of material and laser parameters for low energy consuming and highly efficient devices based on TIMS in nanomagnets. Importantly, our study predicts that the electron-phonon coupling constant, whose value is in general not accurately known, becomes a vital factor in engineering materials and structures for TIMS.

This work was supported by the European Community's Seventh Framework Programme (FP7/2007-2013) under Grant Agreement No. 281043, FEMTOSPIN. U.A. gratefully acknowledges support from EU FP7 Marie Curie Zukunftskolleg Incoming Fellowship Programme, University of Konstanz (Grant No. 291784). This work made use of the facilities of N8 HPC provided and funded by the N8 consortium and EPSRC (Grant No. EP/K000225/1). The Centre is co-ordinated by the Universities of Leeds and Manchester. O.C.-F. acknowledges the financial support from the Spanish Ministry of Economy and Competitiveness under the Grant MAT2013-47078-C2-2-P.

- ¹S. Mangin, D. Ravelosona, J. A. Katine, M. J. Carey, B. D. Terris, and E. E. Fullerton, *Nat. Mater.* **5**, 210 (2006).
- ²F. Matsukura, Y. Tokura, and H. Ohno, *Nat. Nanotechnol.* **10**, 209 (2015).
- ³V. V. Temnov, *Nat. Photonics* **6**, 728 (2012).
- ⁴G. E. W. Bauer, E. Saitoh, and B. J. van Wees, *Nat. Mater.* **11**, 391 (2012).
- ⁵A. Kirilyuk, A. V. Kimel, and T. Rasing, *Rev. Mod. Phys.* **82**, 2731 (2010).
- ⁶C. D. Stanciu, F. Hansteen, A. V. Kimel, A. Kirilyuk, A. Tsukamoto, A. Itoh, and T. Rasing, *Phys. Rev. Lett.* **99**, 047601 (2007).
- ⁷L. Le Guyader, S. El Moussaoui, M. Buzzi, R. V. Chopdekar, L. J. Heyderman, A. Tsukamoto, A. Itoh, A. Kirilyuk, T. Rasing, and A. V. Kimel, *Appl. Phys. Lett.* **101**, 022410 (2012).
- ⁸Z. Azim, X. Fong, T. Ostler, R. Chantrell, and K. Roy, *IEEE Electron Device Lett.* **35**, 1317 (2014).
- ⁹T. A. Ostler, J. Barker, R. F. L. Evans, R. W. Chantrell, U. Atxitia, O. Chubykalo-Fesenko, S. El Moussaoui, L. Le Guyader, E. Mengotti, and L. J. Heyderman, *Nat. Commun.* **3**, 666 (2012).
- ¹⁰A. R. Khorsand, M. Savoini, A. Kirilyuk, A. V. Kimel, A. Tsukamoto, A. Itoh, and T. Rasing, *Phys. Rev. Lett.* **108**, 127205 (2012).
- ¹¹T. Liu, T. Wang, A. H. Reid, M. Savoini, X. Wu, B. Koene, P. Granitzka, C. Graves, D. Higley, and Z. Chen, *Nano Lett.* **15**(10), 6862–6868 (2015).
- ¹²J. Barker, U. Atxitia, T. A. Ostler, O. Hovorka, O. Chubykalo-Fesenko, and R. W. Chantrell, *Sci. Rep.* **3**, 3262 (2013).
- ¹³E. Oniciuc, L. Stoleriu, D. Cimpoesu, and A. Stancu, *Appl. Phys. Lett.* **104**, 222404 (2014).
- ¹⁴K. L. Wang, J. G. Alzate, and P. K. Amiri, *J. Phys. D: Appl. Phys.* **46**, 074003 (2013).
- ¹⁵M. Madami, M. d'Aquino, G. Gubbiotti, S. Tacchi, C. Serpico, and G. Carlotti, *Phys. Rev. B* **90**, 104405 (2014).
- ¹⁶A. J. Schellekens and B. Koopmans, *Phys. Rev. B* **87**, 020407 (2013).
- ¹⁷J. H. Mentink, J. Hellsvik, D. V. Afanasiev, B. A. Ivanov, A. Kirilyuk, A. V. Kimel, O. Eriksson, M. I. Katsnelson, and T. Rasing, *Phys. Rev. Lett.* **108**, 057202 (2012).
- ¹⁸S. Wienholdt, D. Hinzke, K. Carva, P. M. Oppeneer, and U. Nowak, *Phys. Rev. B* **88**, 020406 (2013).
- ¹⁹S. Mangin, M. Gottwald, C.-H. H. Lambert, D. Steil, V. Uhlí, L. Pang, M. Hehn, S. Alebrand, M. Cinchetti, G. Malinowski, Y. Fainman, M. Aeschlimann, and E. E. Fullerton, *Nat. Mater.* **13**, 286 (2014).

- ²⁰A. Hassdenteufel, J. Schmidt, C. Schubert, B. Hebler, M. Helm, M. Albrecht, and R. Bratschitsch, *Phys. Rev. B* **91**, 104431 (2015).
- ²¹C. D. Stanciu, A. Tsukamoto, A. V. Kimel, F. Hansteen, A. Kirilyuk, A. Itoh, and T. Rasing, *Phys. Rev. Lett.* **99**, 217204 (2007).
- ²²A. Hassdenteufel, B. Hebler, C. Schubert, A. Liebig, M. Teich, M. Helm, M. Aeschlimann, M. Albrecht, and R. Bratschitsch, *Adv. Mater.* **25**, 3122 (2013).
- ²³U. Atxitia, J. Barker, R. W. Chantrell, and O. Chubykalo-Fesenko, *Phys. Rev. B* **89**, 224421 (2014).
- ²⁴T. A. Ostler, R. F. Evans, R. W. Chantrell, U. Atxitia, O. Chubykalo-Fesenko, I. Radu, R. Abrudan, F. Radu, A. Tsukamoto, and A. Itoh, *Phys. Rev. B* **84**, 024407 (2011).
- ²⁵I. Radu, K. Vahaplar, C. Stamm, T. Kachel, N. Pontius, H. A. Dürr, T. A. Ostler, J. Barker, R. F. L. Evans, R. W. Chantrell, A. Tsukamoto, A. Itoh, A. Kirilyuk, T. Rasing, and A. V. Kimel, *Nature* **472**, 205 (2011).
- ²⁶S. I. Anisimov, B. L. Kapeliovich, and T. L. Perelman, *Zh. Eksp. Teor. Fiz.* **66**, 776 (1974) [*Sov. Phys. JETP* **39**(2), 375–377 (1974)].
- ²⁷U. Bovensiepen, *J. Phys.: Condens. Matter* **19**, 083201 (2007).
- ²⁸M. J. Verstraete, *J. Phys.: Condens. Matter* **25**, 136001 (2013).
- ²⁹B. Koopmans, G. Malinowski, F. Dalla Longa, D. Steiauf, M. Fähnle, T. Roth, M. Cinchetti, and M. Aeschlimann, *Nat. Mater.* **9**, 259–265 (2009).
- ³⁰Z. Lin, L. V. Zhigilei, and V. Celli, *Phys. Rev. B* **77**, 075133 (2008).
- ³¹A. P. Caffrey, P. E. Hopkins, J. M. Klopff, and P. M. Norris, *Microscale Thermophys. Eng.* **9**, 365 (2005).
- ³²E. Carpene, E. Mancini, C. Dallera, M. Brenna, E. Puppini, and S. De Silvestri, *Phys. Rev. B* **78**, 174422 (2008).
- ³³P. Nieves, D. Serantes, U. Atxitia, and O. Chubykalo-Fesenko, *Phys. Rev. B* **90**, 104428 (2014).